

## Neural markers of loss aversion in resting-state brain activity

Nicola Canessa<sup>a,b,\*</sup>, Chiara Crespi<sup>b,c</sup>, Gabriel Baud-Bovy<sup>d,e</sup>, Alessandra Dodich<sup>b,e</sup>,  
Andrea Falini<sup>e,f</sup>, Giulia Antonellis<sup>e</sup>, Stefano F. Cappa<sup>a,b</sup>

<sup>a</sup> *NETS Center, Scuola Universitaria Superiore IUSS Pavia, Pavia 27100, Italy*

<sup>b</sup> *Division of Neuroscience, San Raffaele Scientific Institute, Milan 20132, Italy*

<sup>c</sup> *Epidemiology and Health Services, National Research Council, Segrate, Milan 20090, Italy*

<sup>d</sup> *Robotics, Brain, and Cognitive Sciences Unit, Istituto Italiano di Tecnologia, 16163 Genoa, Italy*

<sup>e</sup> *Università Vita-Salute San Raffaele, Milan 20132, Italy*

<sup>f</sup> *Neuroradiology Unit, San Raffaele Scientific Institute, Milan 20132, Italy*

### ARTICLE INFO

#### Keywords:

Neuroeconomics  
Loss Aversion  
Resting-state functional Magnetic Resonance Imaging (rs-fMRI)  
Ventral striatum  
Posterior insula  
Interoception

### ABSTRACT

Neural responses in striatal, limbic and somatosensory brain regions track individual differences in loss aversion, i.e. the higher sensitivity to potential losses compared with equivalent gains in decision-making under risk. The engagement of structures involved in the processing of aversive stimuli and experiences raises a further question, i.e. whether the tendency to avoid losses rather than acquire gains represents a transient fearful overreaction elicited by choice-related information, or rather a stable component of one's own preference function, reflecting a specific pattern of neural activity. We tested the latter hypothesis by assessing in 57 healthy human subjects whether the relationship between behavioral and neural loss aversion holds at rest, i.e. when the BOLD signal is collected during 5 minutes of cross-fixation in the absence of an explicit task. Within the resting-state networks highlighted by a spatial group Independent Component Analysis (gICA), we found a significant correlation between strength of activity and behavioral loss aversion in the left ventral striatum and right posterior insula/supramarginal gyrus, i.e. the very same regions displaying a pattern of neural loss aversion during explicit choices. Cross-study analyses confirmed that this correlation holds when voxels identified by gICA are used as regions of interest in task-related activity and vice versa. These results suggest that the individual degree of (neural) loss aversion represents a stable dimension of decision-making, which reflects in specific metrics of intrinsic brain activity at rest possibly modulating cortical excitability at choice.

### 1. Introduction

When making decisions under risk people typically display different degrees of *loss aversion* (Kahneman and Tversky, 1979), i.e. higher sensitivity to potential losses than equivalent gains. The consequences of this phenomenon have been described in managerial (Jarrow and Zhao, 2006), financial (Haigh and List, 2005) and political (Berejikian and Early, 2013) settings. Individual differences in loss aversion have been related to gender (Schmidt and Traub, 2002), age (Gachter et al., 2007), and genetic factors affecting thalamic norepinephrine transmission (Takahashi et al., 2013), as well as neural activity and structure (Canessa et al., 2013).

Neuroimaging studies have highlighted the role played by two oppositely valenced neural systems in decision-making. An appetitive system involves the ventral striatum in the network of reward-based behavioral learning (Doya, 2008). This structure displays an asymmetric bidirectional response of activation for gains and deactivation

for losses, with the steeper degree of deactivation vs. activation reflecting individual differences in behavioral loss aversion (henceforth “neural loss aversion”; Canessa et al., 2013; Tom et al., 2007). An aversive neural mechanism involves the amygdala, as well as the right posterior insula extending into the supramarginal gyrus (Canessa et al., 2013). These regions, mediating anticipatory responses to aversive events (LeDoux, 2012; Sehlmeier et al., 2009), are more strongly activated for prospective losses than deactivated for gains. In the right parietal operculum and supramarginal gyrus the degree of asymmetry of this response is additionally related to behavioral loss aversion, thus mirroring the pattern of neural loss aversion observed in the striatum. The bidirectional (gain-loss) signals coded by these regions likely converge to downstream processing structures, e.g. posterior medial frontal cortex (Canessa et al., 2009, 2011, 2013; Tom et al., 2007), where they may underpin cost-benefit analyses (Croxson et al., 2009).

Importantly, however, human and animal studies have shown a **more complex pattern in striatal** and limbic responses to anticipated

\* Correspondence to: Scuola Universitaria Superiore IUSS, Piazza della Vittoria 15, 27100 Pavia, Italy.  
E-mail address: [nicola.canessa@iusspavia.it](mailto:nicola.canessa@iusspavia.it) (N. Canessa).

and experienced outcomes. The striatum has been shown to code expectations about punishments in addition to rewards, i.e. an “aversive” prediction error (Seymour et al., 2007; Delgado et al., 2008) contributing to the anticipation of financial losses (Delgado et al., 2011). Moreover, lesional (Kazama et al., 2012) and electrophysiological (Sangha et al., 2013) evidence of reward-related coding in amygdala neurons supports its role in mediating avoidance learning also by predicting relief (Rogan et al., 2005; Seymour et al., 2005). While the observation of mixed appetitive and aversive neuronal responses is consistent with the aforesaid bidirectional gain-loss responses in striatal and insular cortex, further evidence is needed to unveil the role of these regions, as well as their connecting circuitry, in outcome anticipation and loss aversion.

The relationship between loss aversion and the dynamics of regions involved in affective processing highlights a crucial issue for neural and behavioral sciences (Camerer, 2005). Loss aversion may represent either a *stable* expression of preferences or rather the consequence of a *transient* fearful reaction to choice-related information. Answering this question would inform a more general discussion on the meaning of (ir)rationality in human decision-making. Avoiding losses, indeed, may reflect a genuine expression of preference, rather than a transitory judgment error, if the loss-related aversive feeling is long-lasting (Camerer, 2005).

We addressed these issues by investigating a neural signature of loss aversion in resting-state activity, i.e. the intrinsic pattern of brain functioning in the absence of an explicit task. In this condition, slow synchronous fluctuations of the BOLD signal in different resting-state networks (RSNs) underlie default connectivity within and between functionally integrated regions (Fox and Raichle, 2007), i.e. those recruited by specific task-related processing (De Luca et al., 2006). We thus predicted that, among different RSNs highlighted by a group Independent Component Analysis, a significant correlation between behavioral loss aversion and the intensity of brain activity would involve the regions displaying neural loss aversion at choice, thus supporting the view of aversion to losses as a stable outcome of processes anticipating prospective affects and bodily states.

## 2. Materials and methods

### 2.1. Participants, task and experimental procedure

Fifty-seven right-handed (Oldfield, 1971) healthy volunteers (25 females and 32 males; mean age=23.8 years; standard deviation [sd]=1.8 years) participated in the study. None of the subjects had previously participated in our fMRI study on the neural bases of loss aversion (Canessa et al., 2013). Moreover, none of them reported a history of neuropsychiatric conditions or substance abuse, nor was currently taking any medication interfering with cognitive functioning. They gave their written informed consent to the experimental procedure, which was approved by the local Ethics Committee.

Participants performed, outside the MR scanner, a gambling task involving the anticipation of real monetary gains and losses (see Canessa et al. (2013) for a detailed description of the task and experimental paradigm). They were asked to accept or reject a series of 104 mixed gambles offering equal chances (fixed at 50%) to gain or lose different amounts of money, sampled from a symmetrical gain-loss matrix with possible gains and losses being uncorrelated. To avoid possible contaminations of resting-state fMRI data by mental activity related to financial outcomes, they were asked to participate in the behavioral task only after the MRI session. Participants' performance resulted either in the increase or decrease of an initial cash endowment that was delivered at least 1 week before task performance to minimize the perception of “windfall” gains. In addition, they completed the short version of the Temperament and Character Inventory (TCI; Cloninger et al. (1994); Italian translation of the revised-TCI by Martinotti et al. (2008)), which measures four dimensions of person-

ality including reward dependence and harm avoidance (data available from 52 out of 57 subjects who agreed to provide personality measures).

### 2.2. Behavioral analysis

The details of the analysis procedure have been previously reported (Canessa et al., 2013). Briefly, we modeled the probability of accepting the mixed gamble using a logistic psychometric function with separate linear utility functions for gains and losses (Tom et al., 2007):

$$\Pr(Y = 1) = \Psi(U_G(G)P_G + U_L(L)P_L) = \Psi\left(\frac{1}{\nu}(\lambda LP_L + (1 - \lambda)GP_G)\right)$$

where  $\Pr(Y=1)$  is the probability of accepting the gamble,  $\Psi(\theta)=1/(1+e^{-\theta})$  is the logistic function,  $U_G(G)P_G+U_L(L)P_L$  is the expected utility for a mixed gamble, and  $U_G(G)=\lambda_G G$  and  $U_L(L)=\lambda_L L$  are the linear utility functions ( $\lambda_G > 0$ ,  $\lambda_L > 0$ ,  $G > 0$  and  $L < 0$ ). As assumed by Prospect Theory, gains and losses can be weighted differently and the utility functions depend on changes in wealth (gains and losses) rather than on the final state of wealth (Kahneman and Tversky, 1979; Tversky and Kahneman, 1992). As in Tom et al. (2007) and Canessa et al. (2013) we did not include probability weighting functions and used linear utility functions to allow the comparison between studies. This Expected Utility (EU) model can be re-parameterized in terms of weighted average between gains and losses with a loss aversion  $\lambda=\lambda_L/(\lambda_L+\lambda_G)$  and response uncertainty  $\nu=1/(\lambda_L+\lambda_G)$  parameters. The loss aversion parameter  $\lambda$  is closely related to the definition of loss aversion used by Tom et al. (2007) ( $\lambda_L/\lambda_G=\lambda/(1-\lambda)$ ). By definition, this parameter indicates a loss averse subject when its value is larger than 0.5. The response uncertainty parameter corresponds to the inverse of the slope of the psychometric function, and reflects how well the model separates the two possible responses.

To test the significance of the loss aversion parameter we also fitted the simpler Expected Value (EV) model to the responses of the subject:

$$\Pr(Y = 1) = \Psi(\beta EV)$$

where  $EV=P_L L+P_G G$  is the expected value of the gamble. Since the EV model is a special case of the previous EU model with loss aversion parameter corresponding to a loss neutral subject ( $\lambda=0.5$ ) and  $\nu=2/\beta$ , the Likelihood Ratio Test (LRT) between the two models follows a  $\chi^2$  distribution with 1 degree of freedom. To estimate participants' risk aversion, the EV model was extended to include the risk as follows:

$$\Pr(Y = 1|P_G, G, P_L, L) = \Psi(\beta_0 + \beta_1 EV + \beta_2 R)$$

where the risk  $R=(G^2 P_G(1-P_G)+L^2 P_L(1-P_L))^{1/2}$  corresponds to the SD of the possible outcomes of the gamble. In this model, the ‘indifference’ straight line  $EV=\gamma_0+\gamma_R R$  with  $\gamma_0=-\beta_0/\beta_1$  and  $\gamma_R=-\beta_2/\beta_1$  expresses a trade-off between the expected value  $EV$  and the risk  $R$  of the gambles toward which the participant has no preference. A positive slope  $\gamma_R$  indicates a risk-averse person who accepts more risky gambles only with a commensurate increase of their expected value.

### 2.3. Resting-state fMRI data collection

We collected functional T2\*-weighted MR images with a 3 T Philips Achieva scanner (Philips Medical Systems, Best, NL), using an 8-channels Sense head coil (sense reduction factor=2). Functional images were acquired using a T2\*-weighted gradient-echo, echo-planar-imaging (EPI) pulse sequence (36 continuous ascending transverse slices covering the whole brain, tilted 30° downward with respect to the bicommissural line to reduce susceptibility artifacts in orbitofrontal regions; TR=2000 ms, TE=30 ms, flip-angle=85°, FOV=192 mm×192 mm, slice thickness=3.7 mm, interslice gap=0.55 mm, in-plane resolution=2 mm×2 mm). The rs-fMRI session included 150 volumes (corresponding to 5 min), preceded by 6 “dummy” functional volumes covering the amount of time needed to

allow for T1-equilibration effects.

Participants were positioned comfortably on the scanner bed and fitted with soft ear plugs; foam pads were used to minimize head movement. They were then instructed to lie quietly with their eyes open and stare passively at a foveally presented fixation cross. This procedure has been shown to facilitate network delineation compared with eyes-closed conditions (Van Dijk et al., 2010).

#### 2.4. rs-fMRI data pre-processing

Image pre-processing was performed using SPM8 (<http://www.fil.ion.ucl.ac.uk/spm>), implemented in Matlab v7.4 (Mathworks, Inc., Sherborn, MA) (Worsley and Friston, 1995). The 150 volumes from each subject underwent a standard spatial pre-processing including spatial realignment to the first volume and unwarping, slice-timing correction with the middle slice in time as a reference, spatial normalization into the standard Montreal Neurological Institute (MNI) space and resampling in  $2 \times 2 \times 2$  mm<sup>3</sup> voxels, as well as spatial smoothing with a 8 mm full-width half-maximum (FWHM) isotropic Gaussian kernel. We then divided the time series of each voxel by its average intensity, in order to convert them to percent signal change units. This procedure of “intensity normalization” has been shown to improve the accuracy and test-retest reliability of the output components of Independent Component Analysis (ICA) (Allen et al., 2011).

We assessed the consistency of spatial normalization across participants by computing the spatial correlation between the SPM EPI template and the smoothed normalized mean image of the realigned volumes of each subject. Such correlation was above 95% (mean=0.965, SD=0.002) for all participants, indicating a reliable and consistent spatial normalization. In addition, we used the Motion Fingerprint toolbox (<http://www.medizin.uni-tuebingen.de/kinder/en/research/neuroimaging/software/>) to compute, for each subject, a comprehensive indicator of scan-to-scan head motion. All subjects met maximum movement threshold of < 1.5 mm in any direction to be included in the analyses (mean=0.66 mm; SD=0.28).

#### 2.5. Group Independent Component Analysis (gICA)

We used multivariate spatial group ICA, as implemented in the GIFT toolbox (<http://icatb.sourceforge.net>; Calhoun et al., 2001), to extract temporally coherent and maximally independent spatial sources, i.e. functional networks or “spatial maps” (SM), from resting-state time series (or timecourses, TCs). ICA was preceded by a data-reduction Principal Component Analysis (PCA) retaining 100 principal components from single subjects’ TCs (Erhardt et al., 2011). Subsequent group ICA retained 75 components through a neural network algorithm (Infomax) that attempts to minimize the mutual information of the network outputs to identify naturally grouping and maximally independent sources (Bell and Sejnowski, 1995). ICA was repeated 250 times in Icasto (<http://research.ics.aalto.fi/ica/icasso/>) and resulting components were clustered to ensure the consistency and reliability of the decomposition, that are quantified using a quality index *I*<sub>q</sub> ranging from 0 to 1 and reflecting the difference between intra-cluster and extra-cluster similarity (Himberg et al., 2004). Aggregate SMs were estimated as the centropotypes of component clusters to reduce sensitivity to initial algorithms parameters. Subject-specific SMs and TCs were estimated with gICA3 back-reconstruction (Calhoun et al., 2001; Erhardt et al., 2011).

##### 2.5.1. RSN selection and identification

We used the spectral characteristics of component TCs to discriminate RSNs from physiological artefacts. Based on the notion that resting-state TCs are dominated by low frequency fluctuations (Cordes et al., 2000), following Allen et al. (2011) we focused on two complementary metrics related to the average power spectrum of

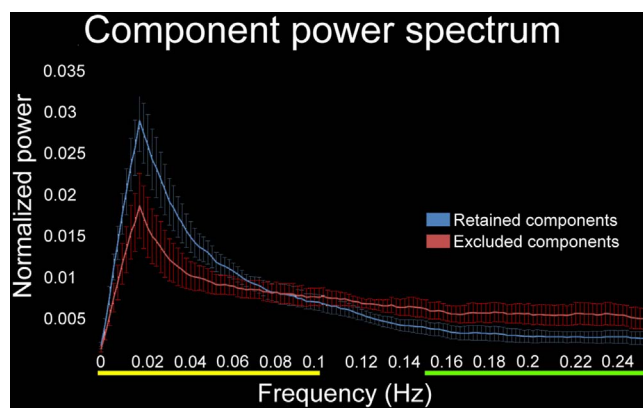


**Fig. 1.** Spectral properties of retained and excluded resting-state Independent Components. Average power spectrum of both the retained ( $n=35$ ; blue) and excluded ( $n=40$ ; red) independent components (ICs), showing the mean ( $\pm$  standard deviation) contribution of each of 129 frequency bins (horizontal axis; range=0–0.25 Hz) to normalized power (vertical axis). Components were selected based on “dynamic range”, i.e. the difference between peak power and minimum power at frequencies to the right of the peak, and “low frequency to high frequency power ratio”, i.e. the ratio of the integral of spectral power below 0.1 Hz (low frequencies; yellow sector) to the integral of power between 0.15 and 0.25 Hz (high frequencies; green sector).

components (Fig. 1). The first is the “dynamic range”, i.e. the difference between peak power and minimum power at frequencies to the right of the peak. The second is “low frequency to high frequency power ratio”, i.e. the ratio of the integral of spectral power below 0.1 Hz to the integral of power between 0.15 and 0.25 Hz (low and high frequencies respectively). In addition, the aggregate spatial maps underwent a visual inspection by three independent raters, based on expectations that they should involve grey matter rather than known ventricular, vascular, susceptibility or motion-related artefacts. Each rater scored spatial maps by assigning them to one of three possible classes, i.e. definite artefact (0), mixed (1) or genuine resting-state component (2). We retained only the components assigned to the latter class by all raters. The two spectral characteristics, alongside an  $I_q > 0.8$  and the visual inspection of the aggregate SMs, led to identify a subset of 35 out of 75 components as genuine RSNs. We anatomically labelled the retained RSNs using the template provided by the GIFT toolbox. A refined labelling of the components showing a significant relationship with loss aversion (see below) was performed using the cytoarchitectonic maps implemented in the SPM Anatomy toolbox v2.2c [Eickhoff et al., 2005] and the Oxford-GSK-Imanova connectivity striatal atlas [Tziortzi et al., 2014] provided by FSL [[www.fmrib.ox.ac.uk/fsl](http://www.fmrib.ox.ac.uk/fsl)].

##### 2.5.2. Statistical analyses: loss aversion and intensity of intrinsic brain activity

For all the selected components, we then performed correlational analyses to investigate a significant relationship between behavioral loss aversion and the intensity of resting-state spatial maps (SMs), related to the connectivity and degree of coactivation within a network (Allen et al., 2011). Since our previous study had shown a significant positive correlation between loss aversion and risk aversion, we used partial correlations to test this correlation while controlling for risk aversion. Component SMs were thresholded based on the distribution of voxelwise *t*-statistics (mean+4 SD) in order to identify voxels with strong and consistent activation across subjects and thus focus subsequent analyses on the most representative sectors of each network. Although spatial ICA successfully identifies motion-related sources which are removed from analyses (McKeown et al., 2003; Kochiyama et al., 2005), we included average scan-to-scan motion as a nuisance predictor in order to discount any residual motion-related variance in RSNs.

We report as statistically significant only the results surviving a  $p < 0.05$  threshold corrected for multiple comparisons using False

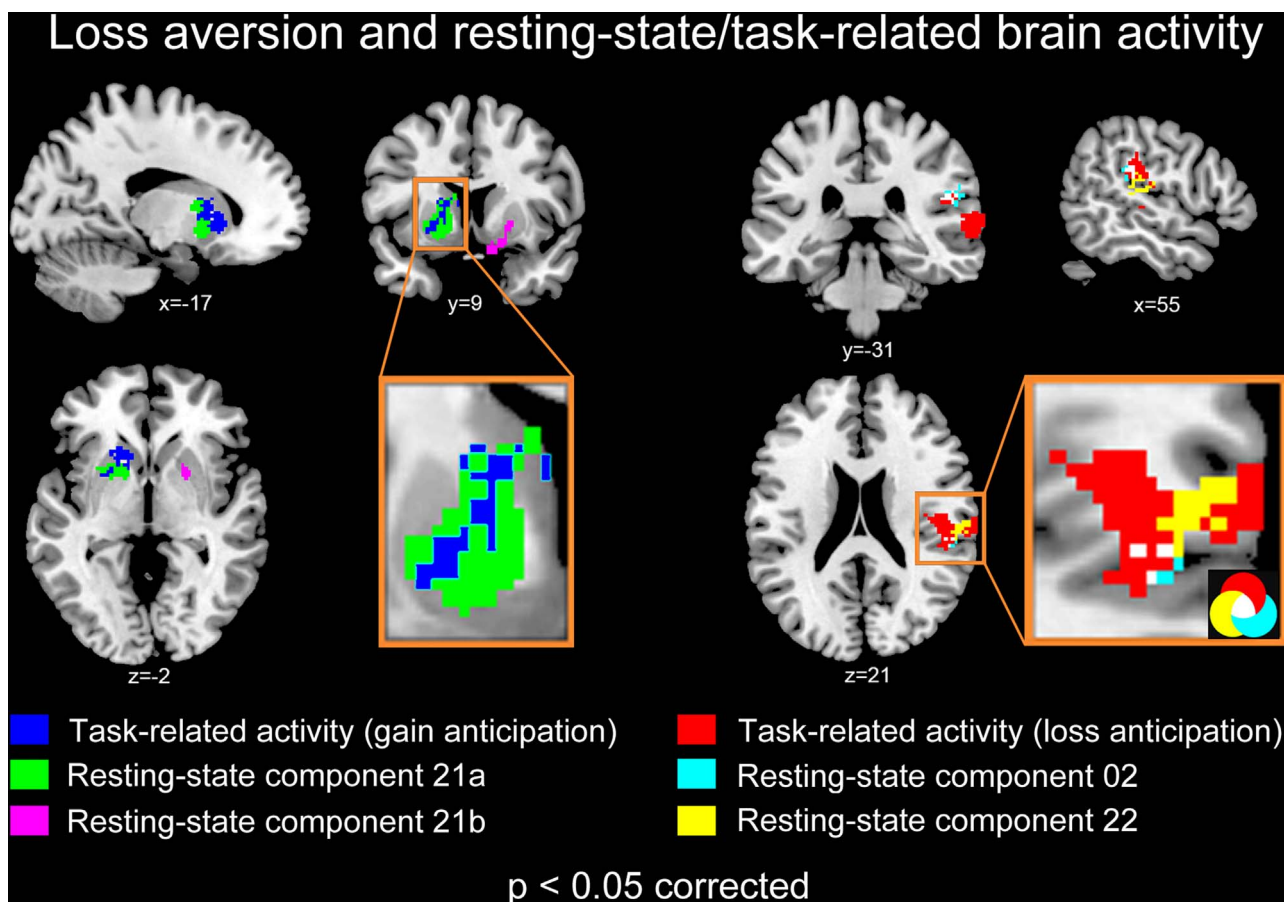


**Fig. 2.** Loss aversion and resting-state/task-related brain activity. Loss aversion, i.e. the overweighting of prospective losses compared with equivalent gains in decision-making under risk, is significantly related to spontaneous brain activity in the striatum (IC 21, involving both the left (green) and right (magenta) hemispheres), as well as the right posterior insula (IC 02, cyan) extending into the supramarginal gyrus and lateral temporal cortex (IC 22, yellow). The figure also reports the voxels in which brain activity at choice tracks the amount of anticipated gains in the ventral striatum (blue) and anticipated losses in the right posterior insula/supramarginal gyrus (red), as described by Canessa et al. (2013).

Discovery Rate (FDR; Genovese et al., 2002). In the GIFT toolbox, this equals correcting for the multiple tests performed over all modelled components and retained voxels.

### 2.5.3. Cross-study region-of-interest analyses

We employed cross-study region-of-interest analyses to test the consistency of the present results against our previous data on the neural bases of loss aversion during actual choices (Canessa et al., 2013).

To this purpose, we first used the SPM toolbox Marsbar (<http://marsbar.sourceforge.net/>) to create binary masks of the clusters displaying a significant correlation between the intensity of resting-state brain activity and behavioral loss aversion in the present data. We then used these masks as regions of interest to extract, with the SPM toolbox REX (<http://web.mit.edu/swg/software.htm>), task-related mean parameter estimates from the statistical maps of the 56 subjects participating in the study by Canessa et al. (2013), for subsequent offline correlation analyses. Namely, we tested whether a pattern of neural loss aversion (i.e. correlation between loss aversion and the degree of asymmetry between neural responses to losses vs. gains) holds also in the clusters identified by resting-state correlational analyses. We then performed the reverse procedure, to test whether the correlation between behavioral loss aversion and the intensity of resting-state brain activity holds in the peak-coordinates of the most representative clusters displaying neural loss aversion in our previous study, i.e. left ventral striatum (peak coordinates: -16 18 -2, corresponding to present component 21) and right posterior insula/supramarginal gyrus (peak coordinates: 58 -20 16, corresponding to

present component 2) (note that the amygdala did not display such a response). This cannot be considered an instance of “double-dipping” (Kriegeskorte et al., 2009), since the cross-correlations are computed between voxels identified in two distinct studies based on different statistical analyses and samples.

In order to test the specificity of such relationship we additionally run all the above analyses as partial correlations, i.e. between brain activity and loss aversion while controlling for risk aversion. In addition, we repeated this procedure to test a correlation between intrinsic brain activity and the *uncertainty* parameter.

We report as statistically significant only the results surviving a  $p < 0.05$  statistical threshold corrected for multiple comparisons based on False Discovery Rate (FDR; Benjamini and Hochberg, 1995).

### 2.5.4. Prediction of loss aversion using intrinsic brain activity

We employed a multiple regression model to assess the global efficacy of intrinsic brain activity for predicting loss aversion, while also further testing the functional overlap between its task-related and resting-state neural correlates. To this purpose, we entered the average intensity of resting-state activity in the left striatal and right posterior insular clusters reported in our previous study, alongside participants' gender, as simultaneous predictors in a multiple regression model predicting loss aversion (and, separately, risk aversion or uncertainty).

### 3. Results

#### 3.1. Behavioral results

In line with previous evidence (e.g. Gächter et al., 2007), 45 subjects (78.9%; 19 females and 26 males) were loss averse (LRT:  $p < 0.05$  and  $\lambda > 0.5$ ), 9 (15.8%; 4 females and 5 males) were loss neutral (LRT:  $p > 0.05$  and  $\lambda \approx 0.5$ ), and 3 (5.2%; 2 females and 1 male) were loss prone (LRT:  $p < 0.05$  and  $\lambda < 0.5$ ). Loss aversion was strongly correlated with risk aversion ( $r=0.902$ ,  $p < 0.00001$ ). There was no significant gender difference in loss aversion ( $t(55)=0.659$ ,  $p=0.512$ ), risk ( $t(55)=0.457$ ,  $p=0.649$ ) or uncertainty ( $t(55)=1.373$ ,  $p=0.175$ ). In addition, we found no significant correlation between loss aversion and any of the temperament TCI scales (harm avoidance, reward dependence, novelty seeking and persistence; all  $p > 0.1$ ). In keeping with our previous data (Canessa et al., 2013) behavioral loss aversion was negatively related to the overall payoff ( $r=-0.475$ ,  $p=0.000188$ ).

#### 3.2. Loss aversion and intensity of resting-state brain activity

We observed a significant positive correlation between behavioral loss aversion and the intensity of intrinsic brain activity in three components, involving the ventral striatum bilaterally (component 21; simple correlation:  $r=0.6103$ ,  $r^2=0.3724$ , FDR- $p < 0.000001$ ; partial correlation with risk:  $r=0.5326$ , FDR- $p=0.000069$ ) as well as the right posterior insular cortex and parietal operculum (component 2; simple correlation:  $r=0.5929$ ,  $r^2=0.3516$ , FDR- $p < 0.000001$ ; partial correlation with risk:  $r=0.2740$ , FDR- $p=0.041$ ) extending laterally into the supramarginal gyrus and lateral temporal cortex (component 22; simple correlation:  $r=0.5203$ ,  $r^2=0.2707$ , FDR- $p < 0.000001$ ; partial correlation with risk:  $r=0.509$ , FDR- $p=0.0000915$ ) (see Fig. 2 and Table 1). Striatal activations encompassed the limbic striatum (mainly the nucleus accumbens) and putamen bilaterally, as well as the caudate in the left hemisphere (Tziortzi et al., 2014). Caudal activations involved the posterior insular cortex and the parietal operculum (OP1/OP2) in the secondary somatosensory cortex (Eickhoff et al., 2006a,b). Only a marginally significant correlation (FDR- $p=0.072$ ) was found for a further cluster encompassing the left amygdala, which was thus excluded from subsequent analyses.

The spatial overlap between these loci of resting-state activity and those observed by Canessa et al. (2013) in subjects making real choices (see Fig. 2) were confirmed by cross-study correlational analyses on the average BOLD signal extracted from different regions of interest. First, behavioral loss aversion was positively related to the intensity of resting-state brain activity in the voxels displaying neural loss aversion in Canessa et al. (2013), i.e. the left ventral striatum (displaying steeper

deactivation for losses than activation for gains; simple correlation:  $r=0.3404$ , FDR- $p=0.0123$ ; partial correlation with risk:  $r=0.3077$ , FDR- $p=0.021$ ) and the right posterior insula/supramarginal gyrus (displaying steeper activation for losses than deactivation for gains; simple correlation:  $r=0.3607$ , FDR- $p=0.0116$ ; partial correlation with risk:  $r=0.3177$ , FDR- $p=0.021$ ) (see Fig. 3; blue and red colors, respectively). Second, a re-analysis of those data confirmed this bidirectional pattern of neural loss aversion also in the left ventral striatum (simple correlation:  $r=0.3323$ , FDR- $p=0.0123$ ; partial correlation with risk:  $r=0.3248$ , FDR- $p=0.021$ ) and right posterior insula/supramarginal gyrus (simple correlation:  $r=0.4710$ , FDR- $p=0.008$ ; partial correlation with risk:  $r=0.4636$ , FDR- $p=0.0012$ ) highlighted by resting-state correlational analyses in the present study (see Fig. 3; green and cyan colors, respectively).

In none of the above analysis, instead, a significant relationship was found between the uncertainty parameter and resting-state brain activity.

Supporting the functional overlap between resting-state and task-related brain activity, a multiple regression model ( $F(3, 53)=6.7359$ ,  $p=0.00062$ ; adjusted  $R^2=0.2350$ ) showed that a significant amount of variance in loss aversion was explained by intrinsic activity in the left striatal ( $\beta=0.3644$ ,  $t(53)=3.1056$ ,  $p=0.0030$ , observed power= $0.8619$ ) and right posterior insular ( $\beta=0.3537$ ,  $t(53)=3.0242$ ,  $p=0.0038$ , observed power= $0.8435$ ) clusters engaged by real choices (Canessa et al., 2013), with no significant effect of gender ( $\beta=0.1948$ ,  $t(53)=1.6596$ ,  $p=0.1029$ , observed power= $0.3706$ ). Compared with this evidence, the same model explained a significant but smaller amount of variance of risk aversion ( $F(3, 53)=3.4652$ ,  $p=0.0224$ ; adjusted  $R^2=0.1166$ ), with only the right posterior insula as significant predictor ( $\beta=0.3053$ ,  $t(53)=2.4298$ ,  $p=0.0185$ , observed power= $0.6648$ ). Instead, it did not explain significantly variation in the uncertainty parameter ( $F(3, 53)=1.2641$ ,  $p=0.2960$ ; adjusted  $R^2=0.0139$ ).

Only for visualization purposes we extracted, and plotted against behavioral loss aversion in Fig. 4, the average intensity of spontaneous activity in the voxels which were commonly activated both in the present and our previous study, i.e. left ventral striatum and right posterior insula/supramarginal gyrus.

Among the four temperament scales in the TCI questionnaires, only harm avoidance displayed a significant correlation with neural metrics, i.e. with the strength of resting-state activity in the right posterior insula/supramarginal gyrus (component 22;  $r=0.3172$ ,  $p=0.022$ ). The specificity of this effect was confirmed by a multiple regression model, retaining this cluster as the only significant predictor of variance in harm avoidance (adjusted  $R^2=0.0826$ ,  $p=0.022$ ).

**Table 1**  
Intensity of intrinsic brain activity and loss aversion.

gICA component	K	x	y	Z	H	Anatomical region	Labeling	T-score
Component 21	274	-20	10	-4	L	Putamen	na	5.17
		-18	6	10	L	Putamen	na	3.55
		-8	4	16	L	Caudate Nucleus	na	3.07
	201	10	12	-14	R	Ventral Striatum	na	4.55
		22	2	-6	R	Pallidum	na	3.58
Component 2	246	50	-26	22	R	Rolandic Operculum	Area OP1 [SII]	4.84
		38	-12	16	R	Insula Lobe	Area OP3 [VS]	3.02
		58	-26	32	R	SupraMarginal Gyrus	Area Pft (IPL)	2.96
Component 22	83	62	-22	20	R	SupraMarginal Gyrus	Area OP1 [SII]	5.35

Anatomical characterization of the gICA components in which the intensity of intrinsic brain activity is significantly related to behavioral loss aversion ( $p < 0.05$  FDR corrected for multiple comparisons). Cytoarchitectonic labeling was performed based on the overlap between each cluster and available probability maps on the Anatomy Toolbox for SPM (v.2.2c; Eickhoff et al., 2005). Striatal activations were localized on the Oxford-GSK-Imanova connectivity striatal atlas [Tziortzi et al., 2014].

K: cluster extent in number of voxels ( $2 \times 2 \times 2 \text{ mm}^3$ ); H: Hemisphere; L: Left; R: right; na: not assigned to any known cytoarchitectonic probability map; OP: parietal operculum; SII: secondary somatosensory; VS: Ventral Somatosensory; IPL: inferior parietal lobule.

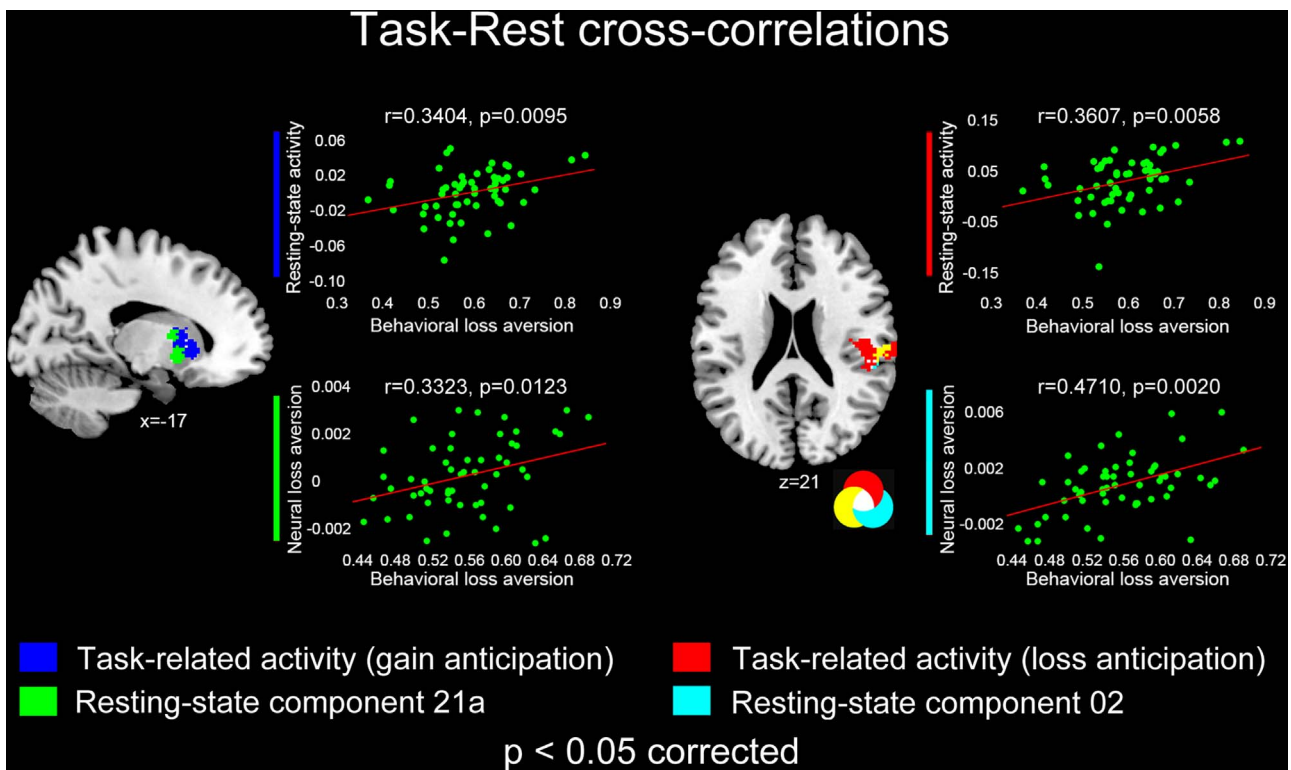


**Fig. 3.** Task-Rest cross-correlations. Top panels: behavioral loss aversion is positively related with the intensity of resting-state brain activity in the voxels displaying neural loss aversion at choice in Canessa et al. (2013), i.e. the left ventral striatum displaying steeper deactivation for losses than activation for gains (blue) and the right posterior insula/supramarginal gyrus displaying steeper activation for losses than deactivation for gains (red). Bottom panels: a re-analysis of our previous data confirmed a bidirectional pattern of neural loss aversion, i.e. different slope in the gain vs. loss responses, also in the left ventral striatum (steeper deactivation for losses than activation for gains; green) and right posterior insula/supramarginal gyrus (steeper activation for losses than deactivation for gains; cyan) voxels highlighted by resting-state correlational analyses in the present study.

#### 4. Discussion

The main aim of this study is to assess whether loss aversion and its associated neural responses are reflecting a transient affective over-reaction to prospective losses, or are rather a genuine expression of a stable preference function (Camerer, 2005). The latter claim would be strongly supported by observing that a neural signature of loss aversion, in the same structures recruited by explicit choices, can be identified even in the intrinsic brain activity of individuals who are not making any decision. Our results confirmed that, even when controlling for the effect of risk aversion, behavioral loss aversion reflects the

intensity of spontaneous brain activity in the same regions displaying neural loss aversion at choice, i.e. left ventral striatum and right posterior insula/supramarginal gyrus (Canessa et al., 2013; Tom et al. 2007), thus supporting the view of aversion to losses as an endogenous feature of human decision-making.

Cross-study correlational analyses confirmed the functional implications of the spatial overlap between the present results and those of our previous study on task-related activations tracking loss aversion. In addition, we found that 23.5% of the variance of subjects' loss aversion was jointly explained by the intensity of *intrinsic brain activity* in the regions which, in our previous study, were associated with neural loss

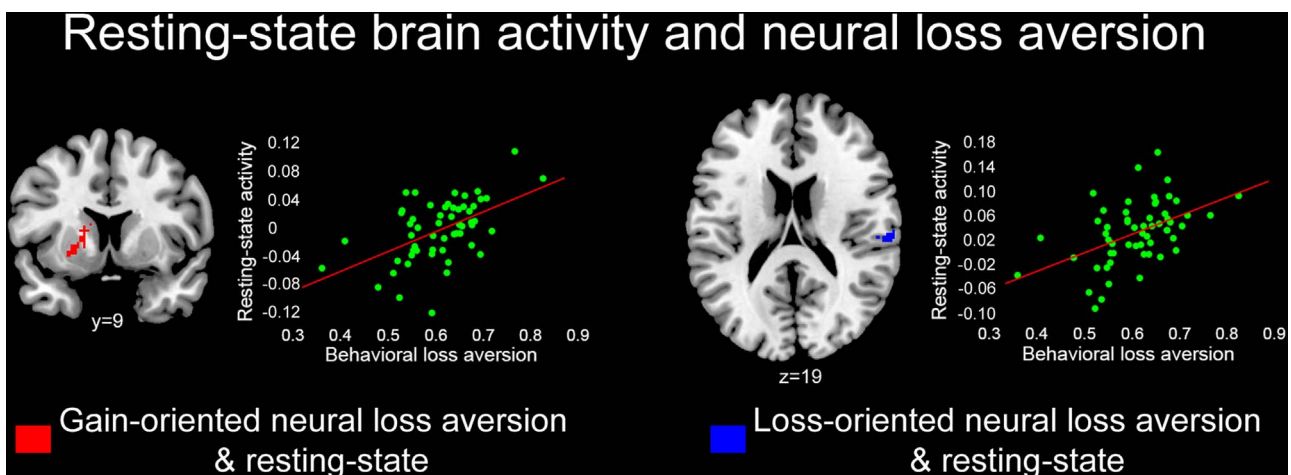


**Fig. 4.** Spatial and functional overlap between intrinsic and task-related brain activity. Behavioral loss aversion is positively related with the intensity of intrinsic brain activity in the common voxels across resting-state and task-related analyses, i.e. the left ventral striatum (red) and right posterior insula/supramarginal gyrus (blue). Scatterplots are for visualization purpose only, and not used for any statistical inference.

aversion during explicit choices, i.e. the left ventral striatum and right posterior insula (Fig. 4). In sum, the consistent relationship between behavioral and neural metrics obtained in different samples and conditions suggests that behavioral loss aversion, as well as neural loss aversion in the left ventral striatum and right posterior insula/supramarginal gyrus, are strongly related with the intensity of resting-state activity in these very same brain structures.

This evidence may provide insights into the nature and the neural mechanisms of loss aversion. Previous studies have shown that resting-state brain activity reflects intrinsic brain connectivity between and within *functional networks*, i.e. groups of regions supporting cognitive and sensorimotor performance beyond rest (De Luca et al., 2006). The intrinsic functional architecture of the resting brain may thus unveil a *baseline* level of the neurophysiological mechanisms underlying cognitive functioning, unbiased by factors possibly affecting task-related brain activity. Several studies have started to address the relationship between different metrics of resting-state brain activity (reflecting complementary facets of functional connectivity; Allen et al., 2011) and several cognitive, sensorimotor or behavioral variables. Preliminary neuroeconomic evidence in healthy individuals has related individual differences in risk-seeking to intrinsic brain activity in the medial orbitofrontal cortex (Neubert et al., 2015), right inferior frontal cortex (Cox et al., 2010; Gianotti et al., 2009; Zhou et al., 2014) and striatum (Cox et al., 2010). Extending these results, here we show that loss aversion reflects in higher spontaneous brain activity in the *same* regions coding a disproportionate neural anticipation of losses vs. gains when making real choices.

By using a blind ICA approach to investigate a relationship between loss aversion and *structural architecture*, we had already shown that the former correlates with grey matter volume in a network encompassing the striatum, as well as amygdala and thalamus (Canessa et al., 2013). Those data supported the view of loss aversion as a stable behavioral response reflecting the structural properties of the network of reinforcement learning (Doya, 2008). The present results additionally show that aversion to losses reflects an intrinsic *functional architecture*, thus grounding (neural) loss aversion in the *intrinsic connectivity* of brain regions in charge of anticipating and evaluating prospective outcomes. These results raise further crucial issues concerning the functional significance of this evidence for the neural mechanisms underlying actual choices, and more generally the dynamic functional role of spontaneous activity at rest. The fact that visuo-perceptual learning modifies the resting covariance structure of spontaneous activity between networks engaged by the task (Lewis et al., 2009) suggests that such activity plays a role in maintaining ongoing representations of the relationship between sensory stimuli and behavioral responses. The present results extend these observations to the decisional domain, supporting the notion that the neural mechanisms underlying choice are not a *passive sensory-motor analyzer driven by environmental stimuli* (Lewis et al., 2009). They may actually maintain an active representation of the value associated to different options (e.g. gains vs. losses or sure vs. risky), shaped both from a genetic disposition (Voigt et al., 2015) and prior experience. Our results show that, in the case of outcome anticipation and loss aversion, this neural representation involves the left ventral striatum and right posterior insula/supramarginal gyrus. The relationship between neural and behavioral loss aversion observed in these structures at rest may reflect their baseline level of spontaneous activity, in turn modulating their reactivity under cognitive and affective stimulation.

This hypothesis highlights a possible interpretation of (neural) loss aversion in terms of increased prediction of an aversive body state, associated with heightened anxious affects and driven by a network centered on the striatum and insular cortex (Paulus and Stein, 2006). Growing evidence shows that the latter underpins a sense of the physiological condition of the body (Craig, 2002), through the integration of primary somato-visceral signals in the posterior insula and their convergence to a representation of the internal bodily state generated

in the right anterior insula. Recent models suggest that, via associative mechanisms analogous to those described in the mesolimbic dopaminergic pathway (Schultz, 2007), this circuitry also underpins the generation of *anticipatory* signals related to prospective negative outcomes (Ploghaus et al., 1999), neurally embodied as aversive bodily states. This process is strictly dependent on bidirectional anatomical connections between the insular cortex and other key structures of adaptive behavioral learning, i.e. the nucleus accumbens and amygdala (Reynolds and Zahm, 2005), as well as the orbitofrontal cortex (Ongur and Price, 2000).

Importantly, however, while both the striatum and posterior insula mediate individual differences in loss aversion, the latter also contributes - although to a smaller extent - to risk aversion. This functional heterogeneity suggests that these structures play different roles. The striatum is a core component of the network underlying outcome anticipation in decision-making under risk (Tom et al., 2007; Knutson and Huettel, 2015). Increasing evidence, however, shows that rather than being a mere “reward” center the striatum may drive connections between the cortical and subcortical nodes of the networks underlying action selection in order to increase the efficiency and vigor of avoidance, in addition to approach, behavior (Floresco, 2015). Within this circuitry, the insula integrates and updates information about the aversive vs. appetitive value of stimuli, in order to predict their effects on prospective body states (Paulus and Stein, 2006). The connections between anterior insula and anterior cingulate cortex may then underpin the allocation of attentional resources and behavioral adaptations to such stimuli by executive processes of cognitive control (Ridderinkhof et al., 2004).

It has been suggested that this model of interoception accounts for “anxiety sensitivity”, i.e. the tendency of some individuals to perceive interoceptive signals as threatening, mediated by heightened insular aversive prediction signals alongside enhanced signaling of saliency by the amygdala (Paulus and Stein, 2006). Supporting this view, several studies highlighted increased insular activity in anxiety disorders, e.g. during symptom provocation (Rauch et al., 1997), observation of fearful faces (Wright et al., 2003) or anticipation of aversive stimuli (Simmons et al., 2006), in phobic patients. A neural signature of anxiety has been found also in resting-state brain activity, with abnormal amygdala-insula connectivity tracking both state-anxiety (the discomfort induced temporarily by situations perceived as dangerous) and trait-anxiety (a relatively enduring disposition to feel stress, worry, and discomfort) (Dennis et al., 2011). In line with this literature, our finding of a positive correlation between intrinsic posterior insular activity and harm avoidance supports previous evidence showing that insular activity during risky choices tracks the perception of homeostatic imbalance (Droutman et al., 2015) and stable traits such as neuroticism (Paulus et al., 2003). Although we found no direct relationship between harm avoidance and loss aversion, our data thus highlight a connection between their neural underpinnings. Namely, in line with previous data they suggest that personality traits related to anxious affects and anticipatory worries emerge from the spontaneous activity of neural regions in which aversive interoceptive signals provide a powerful mean for anticipated emotions to modulate cognitive processing and behavioral responses (Mellers et al., 1999), typically leading to avoidance of risk and conservative choices.

A limitation of this study is represented by the restricted age range and background of participants, most of whom were university students. Although with conflicting results, decision-making has been shown to be influenced by socio-economic status (Hall et al., 2014; Shah et al., 2015), cognitive abilities and education status (Cokely and Kelley, 2009; Klein, 1999), as well as age-associated declines in dopaminergic and serotonergic neuromodulation (Eppinger et al., 2011; Rutledge et al., 2016). Further studies should thus assess the extent to which our findings can be generalized to different subject samples.

## 5. Conclusions

Our results thus support the view of loss aversion as a stable expression of preferences (Camerer, 2005), encoded in the *functional and structural architecture* of a limbic-somatosensory neural system anticipating heightened aversive bodily states. Even when no choice is required, individual differences in the spontaneous responsiveness of this interoceptive system reflect the impact of anticipated negative affects on evaluative processes, leading to avoid losses rather than acquire greater but risky gains. Such an account of (neural) loss aversion in terms of increased prediction of aversive bodily states closely mirrors its interpretation as an *affective forecasting error* highlighted by psychological studies (Kermer et al., 2006). The latter have shown that losses loom larger than gains in prospect even more than in reality, because people overestimate the intensity and duration of their reactions to negative outcomes (i.e. *impact bias*; Kahneman and Snell, 1992), as well as the degree to which their future states will resemble their current states (*projection bias*; Loewenstein et al., 2003).

While providing novel evidence on the neural mechanisms underpinning decision-making under risk, these data highlight possible directions for the future investigation of choice mechanisms in health and disease.

## Acknowledgments

We wish to thank the Center for Excellence in High Field Magnetic Resonance Imaging (CERMAC) of San Raffaele Scientific Institute for supporting this study. The authors declare no competing financial interests.

## References

- Allen, E.A., Erhardt, E.B., Damaraju, E., Gruner, W., Segall, J.M., Silva, R.F., Havlicek, M., Rachakonda, S., Fries, J., Kalyanam, R., Michael, A.M., Caprihan, A., Turner, J.A., Eichele, T., Adelsheim, S., Bryan, A.D., Bustillo, J., Clark, V.P., Feldstein Ewing, S.W., Filbey, F., Ford, C.C., Hutchison, K., Jung, R.E., Kiehl, K.A., Kodituwakku, P., Komesu, Y.M., Mayer, A.R., Pearson, G.D., Phillips, J.P., Sadek, J.R., Stevens, M., Teuscher, U., Thoma, R.J., Calhoun, V.D., 2011. A baseline for the multivariate comparison of resting-state networks. *Front Syst. Neurosci.* 5, 2.
- Bell, A.J., Sejnowski, T.J., 1995. An information-maximization approach to blind separation and blind deconvolution. *Neural Comput.* 7, 1129–1159.
- Benjamini, Y., Hochberg, Y., 1995. Controlling the false discovery rate: a practical and powerful approach to multiple testing. *J. R. Stat. Soc.* 57, 289–300.
- Berejikian, J.D., Early, B.R., 2013. Loss Aversion and Foreign Policy Resolve. *Political Psychol.* 34, 649–671.
- Calhoun, V.D., Adali, T., Pearson, G.D., Pekar, J.J., 2001. A method for making group inferences from functional MRI data using independent component analysis. *Hum. Brain Mapp.* 14, 140–151.
- Camerer, C., 2005. Three Cheers—Psychological, Theoretical, Empirical—For Loss Aversion. *J. Mark. Res.* 42, 129–133.
- Canessa, N., Motterlini, M., Alemanno, F., Perani, D., Cappa, S.F., 2011. Learning from other people's experience: a neuroimaging study of decisional interactive-learning. *Neuroimage* 55, 353–362.
- Canessa, N., Motterlini, M., Di Dio, C., Perani, D., Scifo, P., Cappa, S.F., Rizzolatti, G., 2009. Understanding others' regret: a fMRI study. *PLoS One* 4, e7402.
- Canessa, N., Crespi, C., Motterlini, M., Baud-Bovy, G., Chierchia, G., Pantaleo, G., Tettamanti, M., Cappa, S.F., 2013. The functional and structural neural basis of individual differences in loss aversion. *J. Neurosci.* 33, 14307–14317.
- Cloninger, C.R., Przybeck, T.R., Svrakic, D.M., Wetzel, R.D., 1994. The Temperament and Character Inventory (TCI): a guide to its development and use. St. Louis, MO: center for. *Psychobiol. Pers.*, Wash. Univ.
- Cokely, E.T., Kelley, C.M., 2009. Cognitive abilities and superior decision making under risk: a protocol analysis and process model evaluation. *Judgm. Decis. Mak.* 4, 20–33.
- Cordes, D., Haughton, V.M., Arfanakis, K., Wendt, G.J., Turski, P.A., Moritz, C.H., Quigley, M.A., Meyerand, M.E., 2000. Mapping functionally related regions of brain with functional connectivity MR imaging. *AJNR Am. J. Neuroradiol.* 21, 1636–1644.
- Cox, C.L., Gotimer, K., Roy, A.K., Castellanos, F.X., Milham, M.P., Kelly, C., 2010. Your resting brain CAREs about your risky behavior. *PLoS One* 5, e12296.
- Craig, A.D., 2002. How do you feel? Interoception: the sense of the physiological condition of the body. *Nat. Rev. Neurosci.* 3, 655–666.
- Croxson, P.L., Walton, M.E., O'Reilly, J.X., Behrens, T.E., Rushworth, M.F., 2009. Effort-based cost-benefit valuation and the human brain. *J. Neurosci.* 29, 4531–4541.
- De Luca, M., Beckmann, C.F., De Stefano, N., Matthews, P.M., Smith, S.M., 2006. fMRI resting state networks define distinct modes of long-distance interactions in the human brain. *Neuroimage* 29, 1359–1367.
- Delgado, M.R., Jou, R.L., Phelps, E.A., 2011. Neural systems underlying aversive conditioning in humans with primary and secondary reinforcers. *Front Neurosci.* 5, 71.
- Delgado, M.R., Li, J., Schiller, D., Phelps, E.A., 2008. The role of the striatum in aversive learning and aversive prediction errors. *Philos. Trans. R Soc. Lond. B Biol. Sci.* 363, 3787–3800.
- Dennis, E.L., Gotlib, I.H., Thompson, P.M., Thomason, M.E., 2011. Anxiety modulates insula recruitment in resting-state functional magnetic resonance imaging in youth and adults. *Brain Connect* 1, 245–254.
- Doya, K., 2008. Modulators of decision making. *Nat. Neurosci.* 11, 410–416.
- Droutman, V., Bechara, A., Read, S.J., 2015. Roles of the Different Sub-Regions of the Insular Cortex in Various Phases of the Decision-Making Process. *Front Behav. Neurosci.* 9, 309.
- Eickhoff, S.B., Amunts, K., Mohlberg, H., Zilles, K., 2006a. The human parietal operculum. II. Stereotaxic maps and correlation with functional imaging results. *Cereb. Cortex* 16, 268–279.
- Eickhoff, S.B., Schleicher, A., Zilles, K., Amunts, K., 2006b. The human parietal operculum. I. Cytoarchitectonic mapping of subdivisions. *Cereb. Cortex* 16, 254–267.
- Eickhoff, S.B., Stephan, K.E., Mohlberg, H., Grefkes, C., Fink, G.R., Amunts, K., Zilles, K., 2005. A new SPM toolbox for combining probabilistic cytoarchitectonic maps and functional imaging data. *Neuroimage* 25, 1325–1335.
- Eppinger, B., Hammerer, D., Li, S.C., 2011. Neuromodulation of reward-based learning and decision making in human aging. *Ann. NY Acad. Sci.* 1235, 1–17.
- Erhardt, E.B., Rachakonda, S., Bedrick, E.J., Allen, E.A., Adali, T., Calhoun, V.D., 2011. Comparison of multi-subject ICA methods for analysis of fMRI data. *Hum. Brain Mapp.* 32, 2075–2095.
- Floresco, S.B., 2015. The nucleus accumbens: an interface between cognition, emotion, and action. *Annu. Rev. Psychol.* 66, 25–52.
- Fox, M.D., Raichle, M.E., 2007. Spontaneous fluctuations in brain activity observed with functional magnetic resonance imaging. *Nat. Rev. Neurosci.* 8, 700–711.
- Gachter, S., Johnson, E.J., Hermann, A., 2007. Individual-level loss aversion in riskless and risky choices. *IZA Discuss. Pap. No.* 2961.
- Genovese, C.R., Lazar, N.A., Nichols, T., 2002. Thresholding of statistical maps in functional neuroimaging using the false discovery rate. *Neuroimage* 15, 870–878.
- Gianotti, L.R., Knoch, D., Faber, P.L., Lehmann, D., Pascual-Marqui, R.D., Diezi, C., Schoch, C., Eisenegger, C., Fehr, E., 2009. Tonic activity level in the right prefrontal cortex predicts individuals' risk taking. *Psychol. Sci.* 20, 33–38.
- Haigh, M.S., List, J.A., 2005. Do Professional Traders Exhibit Myopic Loss Aversion? An Experimental Analysis. *J. Financ.* 60, 523–534.
- Hall, C.C., Zhao, J., Shafir, E., 2014. Self-affirmation among the poor: cognitive and behavioral implications. *Psychol. Sci.* 25, 619–625.
- Himberg, J., Hyvarinen, A., Esposito, F., 2004. Validating the independent components of neuroimaging time series via clustering and visualization. *Neuroimage* 22, 1214–1222.
- Jarrow, R., Zhao, F., 2006. Downside Loss Aversion and Portfolio Management. *Manag. Sci.* 52, 558–566.
- Kahneman, D., Tversky, A., 1979. Prospect Theory: an Analysis of Decision under Risk. *Econometrica* 47, 263–291.
- Kahneman, D., Snell, J., 1992. Predicting a changing taste: do people know what they will like? *J. Behav. Decis. Mak.* 5, 187–200.
- Kazama, A.M., Heuer, E., Davis, M., Bachevalier, J., 2012. Effects of neonatal amygdala lesions on fear learning, conditioned inhibition, and extinction in adult macaques. *Behav. Neurosci.* 126, 392–403.
- Kermer, D.A., Driver-Linn, E., Wilson, T.D., Gilbert, D.T., 2006. Loss aversion is an affective forecasting error. *Psychol. Sci.* 17, 649–653.
- Klein, J., 1999. The Relationship between Level of Academic Education and Reversible and Irreversible Processes of Probability Decision-Making. *High. Educ.* 37, 323–339.
- Knutson, B., Huettel, S.A., 2015. The risk matrix. *Curr. Opin. Behav. Sci.* 5, 141–146.
- Kochiyama, T., Morita, T., Okada, T., Yonekura, Y., Matsumura, M., Sadato, N., 2005. Removing the effects of task-related motion using independent-component analysis. *Neuroimage* 25, 802–814.
- Kriegeskorte, N., Simmons, W.K., Bellgowan, P.S., Baker, C.I., 2009. Circular analysis in systems neuroscience: the dangers of double dipping. *Nat. Neurosci.* 12, 535–540.
- LeDoux, J., 2012. Rethinking the emotional brain. *Neuron* 73, 653–676.
- Lewis, C.M., Baldassarre, A., Committer, G., Romani, G.L., Corbetta, M., 2009. Learning sculpts the spontaneous activity of the resting human brain. *Proc. Natl. Acad. Sci. USA* 106, 17558–17563.
- Loewenstein, G., O'Donoghue, T., Rabin, M., 2003. Projection Bias in Predicting Future Utility. *Q. J. Econ.* 118, 1209–1248.
- Martinotti, G., Mandelli, L., Di Nicola, M., Serretti, A., Fossati, A., Borroni, S., Cloninger, C.R., Janiri, L., 2008. Psychometric characteristic of the Italian version of the Temperament and Character Inventory—revised, personality, psychopathology, and attachment styles. *Compr. Psychiatry* 49, 514–522.
- McKeown, M.J., Hansen, L.K., Sejnowski, T.J., 2003. Independent component analysis of functional MRI: what is signal and what is noise? *Curr. Opin. Neurobiol.* 13, 620–629.
- Mellers, B., Schwartz, A., Ritov, I., 1999. Emotion-based choice. *J. Exp. Psychol.: General* 128, 332–345.
- Neubert, F.X., Mars, R.B., Sallet, J., Rushworth, M.F., 2015. Connectivity reveals relationship of brain areas for reward-guided learning and decision making in human and monkey frontal cortex. *Proc. Natl. Acad. Sci. USA* 112, E2695–E2704.
- Oldfield, R.C., 1971. The assessment and analysis of handedness: the Edinburgh inventory. *Neuropsychologia* 9, 97–113.
- Ongur, D., Price, J.L., 2000. The organization of networks within the orbital and medial

- prefrontal cortex of rats, monkeys and humans. *Cereb. Cortex* 10, 206–219.
- Paulus, M.P., Stein, M.B., 2006. An insular view of anxiety. *Biol. Psychiatry* 60, 383–387.
- Paulus, M.P., Rogalsky, C., Simmons, A., Feinstein, J.S., Stein, M.B., 2003. Increased activation in the right insula during risk-taking decision making is related to harm avoidance and neuroticism. *Neuroimage* 19, 1439–1448.
- Ploghaus, A., Tracey, I., Gati, J.S., Clare, S., Menon, R.S., Matthews, P.M., Rawlins, J.N., 1999. Dissociating pain from its anticipation in the human brain. *Science* 284, 1979–1981.
- Rauch, S.L., Savage, C.R., Alpert, N.M., Fischman, A.J., Jenike, M.A., 1997. The functional neuroanatomy of anxiety: a study of three disorders using positron emission tomography and symptom provocation. *Biol. Psychiatry* 42, 446–452.
- Reynolds, S.M., Zahm, D.S., 2005. Specificity in the projections of prefrontal and insular cortex to ventral striatopallidum and the extended amygdala. *J. Neurosci.* 25, 11757–11767.
- Ridderinkhof, K.R., Ullsperger, M., Crone, E.A., Nieuwenhuis, S., 2004. The role of the medial frontal cortex in cognitive control. *Science* 306, 443–447.
- Rogan, M.T., Leon, K.S., Perez, D.L., Kandel, E.R., 2005. Distinct neural signatures for safety and danger in the amygdala and striatum of the mouse. *Neuron* 46, 309–320.
- Rutledge, R.B., Smittenaar, P., Zeidman, P., Brown, H.R., Adams, R.A., Lindenberger, U., Dayan, P., Dolan, R.J., 2016. Risk Taking for Potential Reward Decreases across the Lifespan. *Curr. Biol.* 26, 1634–1639.
- Sangha, S., Chadick, J.Z., Janak, P.H., 2013. Safety encoding in the basal amygdala. *J. Neurosci.* 33, 3744–3751.
- Schmidt, U., Traub, S., 2002. An Experimental Test of Loss Aversion. *J. Risk Uncertain.* 25, 233–249.
- Schultz, W., 2007. Behavioral dopamine signals. *Trends Neurosci.* 30, 203–210.
- Sehlmeyer, C., Schoning, S., Zwitserlood, P., Pfeleiderer, B., Kircher, T., Arolt, V., Konrad, C., 2009. Human fear conditioning and extinction in neuroimaging: a systematic review. *PLoS One* 4, e5865.
- Seymour, B., Daw, N., Dayan, P., Singer, T., Dolan, R., 2007. Differential encoding of losses and gains in the human striatum. *J. Neurosci.* 27, 4826–4831.
- Seymour, B., O'Doherty, J.P., Koltzenburg, M., Wiech, K., Frackowiak, R., Friston, K., Dolan, R., 2005. Opponent appetitive-aversive neural processes underlie predictive learning of pain relief. *Nat. Neurosci.* 8, 1234–1240.
- Shah, A.K., Shafir, E., Mullainathan, S., 2015. Scarcity frames value. *Psychol. Sci.* 26, 402–412.
- Simmons, A., Strigo, I., Matthews, S.C., Paulus, M.P., Stein, M.B., 2006. Anticipation of aversive visual stimuli is associated with increased insula activation in anxiety-prone subjects. *Biol. Psychiatry* 60, 402–409.
- Takahashi, H., Fujie, S., Camerer, C., Arakawa, R., Takano, H., Kodaka, F., Matsui, H., Ideno, T., Okubo, S., Takemura, K., Yamada, M., Eguchi, Y., Murai, T., Okubo, Y., Kato, M., Ito, H., Suhara, T., 2013. Norepinephrine in the brain is associated with aversion to financial loss. *Mol. Psychiatry* 18, 3–4.
- Tom, S.M., Fox, C.R., Trepel, C., Poldrack, R.A., 2007. The neural basis of loss aversion in decision-making under risk. *Science* 315, 515–518.
- Tversky, A., Kahneman, D., 1992. Advances in prospect theory: cumulative representation of uncertainty. *J. Risk Uncertain.* 5.
- Tziortzi, A.C., Haber, S.N., Searle, G.E., Tsoumpas, C., Long, C.J., Shotbolt, P., Douaud, G., Jbabdi, S., Behrens, T.E., Rabiner, E.A., Jenkinson, M., Gunn, R.N., 2014. Connectivity-based functional analysis of dopamine release in the striatum using diffusion-weighted MRI and positron emission tomography. *Cereb. Cortex* 24, 1165–1177.
- Van Dijk, K.R., Hedden, T., Venkataraman, A., Evans, K.C., Lazar, S.W., Buckner, R.L., 2010. Intrinsic functional connectivity as a tool for human connectomics: theory, properties, and optimization. *J. Neurophysiol.* 103, 297–321.
- Voigt, G., Montag, C., Markett, S., Reuter, M., 2015. On the genetics of loss aversion: an interaction effect of BDNF Val66Met and DRD2/ANKK1 Taq1a. *Behav. Neurosci.* 129, 801–811.
- Worsley, K.J., Friston, K.J., 1995. Analysis of fMRI time-series revisited—again. *Neuroimage* 2, 173–181.
- Wright, C.I., Martis, B., McMullin, K., Shin, L.M., Rauch, S.L., 2003. Amygdala and insular responses to emotionally valenced human faces in small animal specific phobia. *Biol. Psychiatry* 54, 1067–1076.
- Zhou, Y., Li, S., Dunn, J., Li, H., Qin, W., Zhu, M., Rao, L.L., Song, M., Yu, C., Jiang, T., 2014. The neural correlates of risk propensity in males and females using resting-state fMRI. *Front Behav. Neurosci.* 8, 2.